

Molecular Packing and Dynamics of the Main Chain and Side Chains in Mesomorphic Poly(vinyl ether)s As Revealed by X-ray Scattering, Dielectric Spectroscopy, Solid State ^2H , and ^{13}C -MAS NMR Spectroscopy

C. Hellermark, U. W. Gedde, and A. Hult*

Department of Polymer Technology, Royal Institute of Technology, S-100 44 Stockholm, Sweden

C. Boeffel

Max-Planck-Institut für Polymerforschung, Postfach 3148, D-6500 Mainz, Germany

R. H. Boyd and F. Liu

Department of Materials Science and Engineering, University of Utah, Salt Lake City, Utah 84112

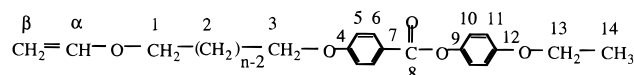
Received April 11, 1996; Revised Manuscript Received March 11, 1998

ABSTRACT: The conformational states and dynamics of a series of side-chain liquid crystalline poly(vinyl ether)s with phenylbenzoate or stilbenzyloxy as mesogen and with 4–11 methylene spacer groups, where the 11-methylene-spacer polymers had two different tacticities, were assessed by dielectric and NMR spectroscopy. Dielectric spectroscopy confirmed the presence of three subglass processes (β , γ , and δ) exhibiting an Arrhenius temperature dependence. The activation energy (35 ± 5 kJ/mol) of the γ process was insensitive to the morphology, and this process is assigned to localized motions within the spacer group. The absence of the β process in the stilbenzyloxy polymer suggests that this process is due to flips of the phenylene units causing a 180° reorientation of the carboxylic group in the phenyl benzoate moiety. The frequency of the flip of the inner phenylene unit at 0°C as obtained by ^{13}C -MAS NMR was almost the same as the frequency of the dielectric β loss peak at the same temperature. The relaxation strength of the β process passed through a maximum as the spacer length increased. It is suggested that the participating carboxyl groups were unable to reorient completely in a polymer with a short spacer group since reorientation of the mesogen was more complete in a polymer with longer spacer groups, the latter containing a smaller percentage of mesogens. ^{13}C -MAS NMR data indicated that the gauche content of the spacer group was lower than that of a free polymethylene chain at the same temperature and that it increased with increasing temperature. The X-ray scattering patterns of the 11-methylene-spacer polymers with different tacticities were identical, and it was shown by NMR and dielectric spectroscopy that the molecular dynamics was not influenced by the tacticity of the polymers. The decrease in the thickness of the smectic layer at the transition from smectic B to smectic A is accompanied by a pronounced increase in segmental mobility of the backbone as revealed by ^2H NMR spectroscopy.

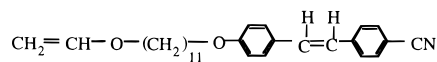
Introduction

The characterization of polymers in the solid state is of great importance in understanding and predicting structure–property relationships. Dielectric spectroscopy is a well-known technique for studying molecular dynamics of polymers. During recent years, solid state ^{13}C -CP-MAS NMR and ^2H NMR spectroscopy have become valuable methods to evaluate chain dynamics and conformational order of polymer chain segments.¹ These methods provide complementary information to X-ray diffraction which can only provide information on the static situation.

Liquid crystalline side-chain poly(vinyl ether)s with different tacticities, ranging from isotactic through atactic to syndiotactic and with spacer groups of different lengths, were prepared by cationic polymerization.^{2–4} It was beforehand believed that the tacticity should play a role in determining the mesomorphic structure, the conformational state, and the thermal transitions. It was however found that the thermal transitions and the smectic layer thicknesses were not significantly affected by the tacticity in the case of the studied liquid crystalline side-chain poly(vinyl ether)s.⁴ This paper presents



Monomer 1



Monomer 2

Figure 1. Structure of vinyl ether monomers **1–n** with numbering of carbon atoms in structures and vinyl ether monomer **2**.

data from dielectric measurements and NMR spectroscopy on the dynamics and conformational states of a range of liquid crystalline side-chain poly(vinyl ether)s at different temperatures. Comparison is made with data obtained by X-ray scattering and differential scanning calorimetry.

Experimental Section

A series of monomers (denoted **1–n**; shown in Figure 1) based on phenyl benzoate as mesogen and ethoxy as terminal group,

* Corresponding author.

and with different methylene spacers having $n = 4, 6, 9, 10$, or 11 were synthesized according to ref 2.

11-(*p*-(4-Ethoxyphenylbenzoate)oxy)undecanylvinyl- d_3 ether (referred to as **1-11D**) with the α and β hydrogens in the backbone replaced by deuterium was prepared according to ref 3, and polymerization was performed according to ref 2. 11-(4'-Cyano-*trans*-4-stilbenzyloxy)undecanyl vinyl ether (denoted as **2**) was synthesized and polymerized as described in a previous paper.⁴ Living polymerization was used, and the resulting poly(**2**) was atactic with a meso-to-racemic dyad ratio close to 2.

The samples were aligned in a 7 T magnetic field by heating to a temperature above the clearing point followed by cooling to a temperature just below the clouding temperature where the sample was kept for 1 h. The samples were finally cooled at a rate of 1 °C/min to room temperature. The order parameter was assessed by analyzing the X-ray scattering pattern.

Differential scanning calorimetry (DSC) was performed using a temperature- and energy-calibrated Perkin-Elmer DSC-7 at heating and cooling rates of 10 °C/min. Hot stage polarized microscopy was carried out in a Leitz Ortholux POL BKII optical microscope equipped with a Mettler hot stage FP 82 controlled by a Mettler FP80 central processor. The 400 MHz ¹H NMR and ¹³C NMR spectra of the monomers and the polymers were recorded in CDCl₃ solution on a Bruker AM-400 spectrometer. IR spectra were obtained using a Perkin-Elmer 1700 FTIR spectrometer.

Solid state ¹³C-CP-MAS NMR experiments were performed on a Bruker MSL300 spectrometer at a ¹H frequency of 300.13 MHz and a ¹³C frequency of 75.47 MHz. The 90° pulse width was 3.7 μ s for both ¹H and ¹³C. Between 512 and 4098 scans were taken with a 3 s repetition time. The experiments were carried out using a double-bearing variable-temperature Bruker MAS probe and 7 mm zirconium oxide rotors.

²H NMR measurements were performed on a Bruker CXP-300 spectrometer operating using a 7 T magnetic field giving a resonance frequency of 45.999 MHz for deuterons. All spectra have been taken with the solid echo pulse sequence using a time delay of 30 μ s between two pulses. The length of the 90° pulse was 2.4 μ s.

The dielectric measurements were made on 25 μ m thick samples with the lateral dimensions 10 mm \times 10 mm held between two rubbed glass plates coated with conductive indium–tin-oxide layers and the polymer (Y type electric cell, E.H.C. Co. Ltd., Japan). The polyimide film showed no measurable dielectric loss in the temperature and frequency range used in this study. The dielectric apparatus was an IMASS TDS time domain spectrometer, based on a design by Mopsik⁵ and equipped with a Hewlett-Packard Series 300 computer. At time $t = 0$, a step voltage of 10 or 100 V was applied between the indium–tin-oxide layers. This caused a charge $Q(t)$ to flow through the sample, and the complex capacitance was obtained as a function of frequency by a numerical Laplace transform, based on a cubic spline, of the time domain capacitance data. The latter covered a time period of 1 min, and frequency domain data were obtained from 10⁻² Hz to 10 kHz. All measurements were carried out by first cooling the sample to -223 °C and then heating it while making measurements at progressively higher temperatures. Temperature equilibrium was established prior to each measurement.

Results and Discussion

The thermal characteristics of the studied monomers and polymers are presented in Tables 1 and 2.

The phase-temperature data presented in Table 2 were based on data obtained by polarized light microscopy and DSC. The assessment of the room-temperature smectic phase of poly(**1-11**) was based on X-ray diffraction analysis of an aligned sample.² Poly(**1-11**) exhibited a hexatic smectic B phase at room temperature which transformed into a smectic A phase at

Table 1. Thermal Transitions in Monomers

monomer	thermal transitions (°C) and corresponding enthalpy changes (J/g) for the monomers, 2nd heating and cooling cycle ^a	
	heating	cooling
1-4	k93(74)i	i82(1.3)n72(57)k
1-6	k82(98)i	i82(4.8)n36(63)k
1-9	k44(5.5)k61 (77)n71(2.3)i	i69(2.2)n55(3.4) _{SA} 34(76)k
1-10	k56(64)n75(3.4)i	i71(3.7)n53(1.6) _{SA} 27(55)k
1-11	k67(70)n76(2.5)i	i70(2.6)n59(3.7) _{SA} 28(60)k
1-11D	k65(88.5)n73(2.5)i	i67(2.6)n57(3.7) _{SA} 28(60)k
2	k99(79)n113(1.8)i	i111(3.5)n79(83)k

^a k, crystalline; _{SA}, smectic A; n, nematic; i, isotropic.

71 °C; the latter was stable up to 140–150 °C after which an isotropic phase was obtained. The majority of the polymers, poly(**1-9**), poly(**1-10**), poly(**1-11**), poly(**1-11D**) and poly(**2**), exhibited enantiotropic mesophases, whereas both poly(**1-4**) and poly(**1-6**) showed monotropic mesophases. Differences in tacticity in poly(**1-11**) and poly(**1-11D**) had no influence on the thermal behavior of these polymers (Table 2). Table 2 also shows that both the phase transition temperatures and enthalpies are considerably lower for poly(**1-10**) than for either poly(**1-9**) or poly(**1-11**).

Figure 2 shows the X-ray diffraction results for poly(**1-11**) expressed as the thickness of the smectic layers obtained from the small-angle reflection and the intermesogenic distance obtained from the wide-angle reflection. A pronounced change in these quantities occurred at temperatures close to 70 °C, which is in agreement with the temperature for the DSC recorded transition between the smectic B and smectic A mesophases (Table 2). The smectic B phase stable at low temperatures is characterized by well-aligned mesogens and a high domain order parameter, which shows up in a high smectic layer thickness and a small average intermesogenic distance (Figure 2).⁶ The reduction in smectic layer thickness by 2 Å and the increase in intermesogenic distance by 0.1 Å accompanying the transition from smectic B to smectic A phase are thus in agreement with the view that the smectic A phase has a lower domain order parameter than the smectic B mesophase.

Figure 3 shows a series of ²H NMR spectra taken at different temperatures of the main-chain deuterated polymer (poly(**1-11D**)) during both heating and cooling periods. At temperatures below the smectic B to smectic A transition, Pake-type spectra were observed, indicating that no motion with correlation times $\tau_c < 10^{-4}$ s took place at the sites of the polymer backbone. The narrow line superimposed in the middle of the spectrum results from mobile terminal groups. A significant narrowing of the lines is observed at the smectic B to smectic A phase transition; cf. heating spectra at temperatures 57 and 67 °C in Figure 3. The spectrum consists of an isotropic line with a line width at half-height of about 17 kHz, which stays almost constant in the smectic phase. At the transition to the isotropic state there is a further decrease of the line width to 1.0 kHz at 157 °C. This line shape is typical for isotropic motions of the polymer backbone. This change in segmental mobility in the backbone is displayed in Figure 4, showing the spectral width at half peak height vs temperature. All spectra showed a superposition of a broad component with a narrow line with a splitting at half-height of less than 1 kHz. This line corresponds

Table 2. Thermal Transitions and Molar Mass Characteristics of Polymers

polymer	\bar{M}_n (g mol ⁻¹)	\bar{M}_w/\bar{M}_n	thermal transitions (°C) and corresponding enthalpy changes (J/g), 2nd heating and cooling cycle ^a	
			heating	cooling
poly(1-4)	12 000	1.9	S _B 99(24)i	i105(0.7)n67(15)S _B
poly(1-6)	11 000	1.7	S _B 77(3.1)n100(1.4)S _A	114(1.4)i i112(1.1)S _A 62(4.1)S _B
poly(1-9)	10 500	1.4	S _B 59 (8.4) S _A 122 (8.8)i	i122(8.6)S _A 52(7.2)S _B
poly(1-10)	10 200	1.5	S _B 45 (5.4)S _A 104 (3.0)i	i 103(4.4)S _A 36(4.0)S _B
poly(1-11)				
<i>m/r</i> = 50/50	12 600	1.7	S _B 71(12)S _A 142(10)i	i131(10.5)S _A 60(12)S _B
<i>m/r</i> = 75/25	13 300	1.7	S _B 73(11)S _A 145(11.4)i	i134(11)S _A 62(11)S _B
poly(1-11D)				
<i>m/r</i> = 50/50	12 500	1.7	S _B 71(10.5)S _A 142(11.6)i	i136(11.6)S _A 64(11.7)S _B
<i>m/r</i> = 75/25	12 000	1.6	S _B 71(10.7)S _A 145(11.4)i	i139(12.2)S _A 65(10.7)S _B
poly(2)	3 600	1.2	k13(5)k32(1.4)SA144(6.5)i	i133(5.9)SA23(12)k

^a k, crystalline; S_B, smectic B; S_A, smectic A; n, nematic; i, isotropic.

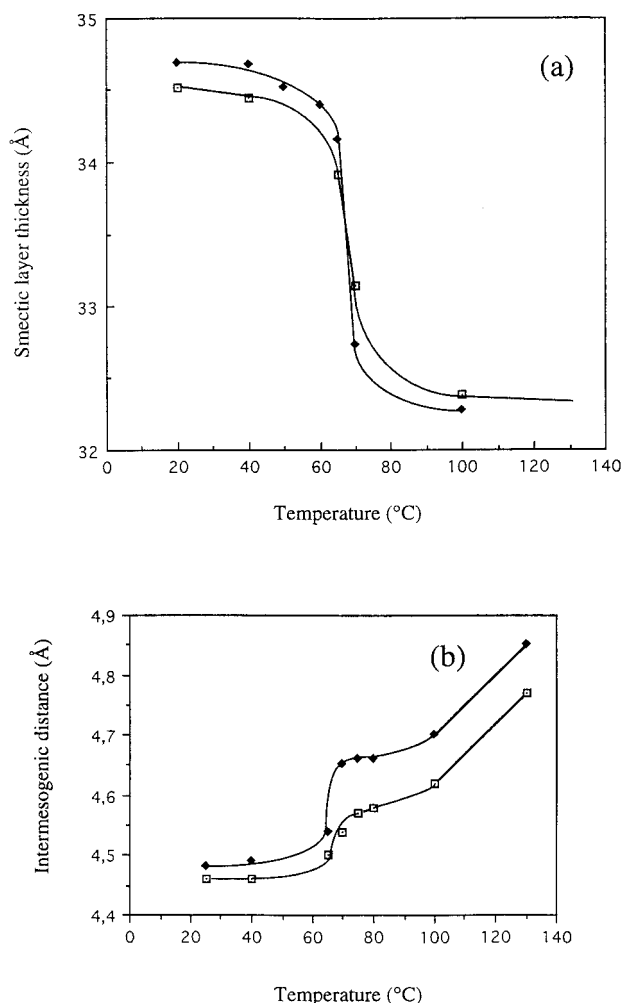


Figure 2. (a) Smectic layer thickness and (b) intermesogenic distance as a function of temperature for oriented isotactic (*m/r* = 75/25; \diamond) and atactic (*m/r* = 50/50; \square) poly(1-11).

to highly mobile methyl end groups with a relative amount of 3% for the polymers studied. Due to the high mobility of these groups over the whole temperature range their existence is visible in all spectra. It should be noted that the structural data from X-ray diffraction presented in Figure 2 and the dynamic data obtained by ²H NMR spectroscopy both exhibit a transition in the same temperature, ca. 65 °C. Poly(1-11D) with different tacticities showed identical ²H NMR spectra, which is the reason why only data for the isotactic polymer are presented here.

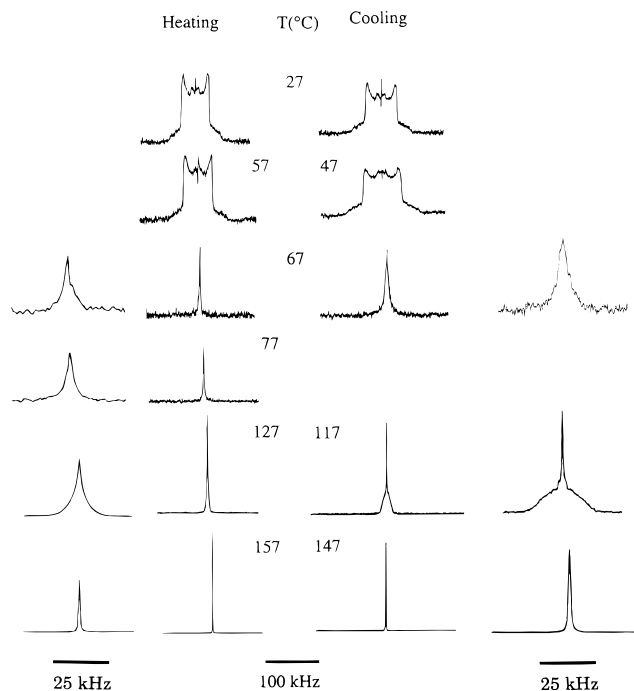


Figure 3. ²H NMR spectra of poly(1-11) (*m/r* = 75/25) recorded at different temperatures as shown in the figure. The outer columns are expansions of the two inner columns. Scale bars are shown under each column.

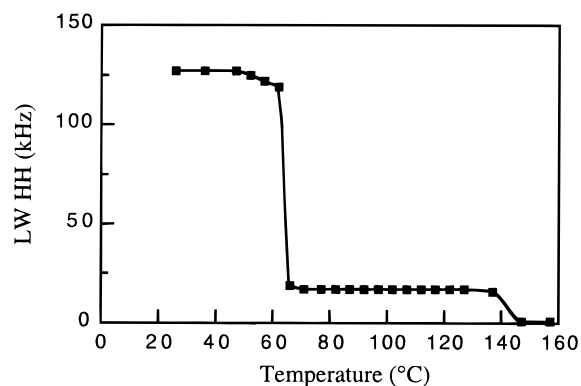


Figure 4. Experimental line width at half peak height (LW HH) vs temperature obtained from the ²H NMR spectra presented in Figure 3 for poly(1-11) with *m/r* = 75/25.

¹³C NMR-CP-MAS-TOSS (total suppression of sidebands) spectra of the isotactic poly(1-11) recorded at different temperatures are shown in Figure 5. At 52 °C, all carbon lines (see Figure 1 for assignment) except



Figure 5. ^{13}C CP MASS TOSS NMR spectra for poly(1-11) ($m/r = 75/25$) recorded at different temperatures as shown in the figure.

for the backbone chain positions are narrow and well resolved due to fast motion in the smectic phase resulting in motionally averaged isotropic chemical shifts. The broad line due to the backbone results from conformational disorder leading to different isotropic chemical shifts. There is no rapid exchange between these different conformations for the polymer backbone at 52 °C, which would lead to an averaging of the isotropic chemical shifts and thus to a line narrowing. This is consistent with the ^2H NMR data where the onset of the motion is only observed at ca. 65 °C (Figure 4). The conformational statistics of the backbone remained constant over the temperature range used in this study (−70 to +52 °C). The spectrum obtained at −70 °C exhibited only broadened lines indicative of packing differences for each position typical for glasses. In a highly ordered crystalline system, narrow lines would be expected, corresponding to positions in their defined crystalline environment. Significant changes with temperature can be observed for mesogenic carbon atoms. The intensity of the peak associated with carbon atom 6 (protonated carbon located in the inner phenylene group; Figure 1) decreased strongly with decreasing temperature, and reached a minimum at about 0 °C. This is an indication that the time scale of the dynamics of the phenylene group was of the same order as the cross polarization time (correlation time $\tau_c \sim (60 \text{ kHz})^{-1}$) at this particular temperature (0 °C). The intensity of

Table 3. Gauche Content in Spacer Group at Room Temperature

polymer	tacticity (m/r)	gauche content (%)
poly(1-11)	75/25	30
poly(1-11)	50/50	22
poly(1-10)	50/50	27
poly(1-9)	50/50	24

the carbon atom 6 peak increased on a further decrease in temperature in indicating freezing of phenylene flip at temperatures ≤ -20 °C (Figure 5). The broadening characteristic of the carbon atom 6 peak at these low temperatures is due to the multitude of frozen-in conformational states leading to a broad distribution of isotropic chemical shifts. A similar temperature dependence was found for the 5/11 carbon peak (protonated carbons located in the inner and outer phenylene groups; Figure 1). These data in conjunction with the data obtained for the carbon atom 6 (inner phenylene) indicate that the two phenylene groups showed similar dynamics. From the signals of the other sites (also including the carboxylic carbon), no conclusion could be drawn about the dynamics of the mesogen. At −70 °C carbon atoms 5 and 11 split into two well-separated lines: $\delta = 110$ and 116 ppm. This splitting is not due to differences of the isotropic chemical shifts, which are calculated to $\delta = 114.1$ and 114.6 ppm for carbons 5 and 11, respectively, but it has to be attributed to a change of the isotropic chemical shifts due to packing effects in the ordered glass. Such effects are usually observed in molecular crystals.

Data for the gauche content in the spacer groups at room temperature for the polymers with different spacer lengths are shown in Table 3. The gauche content was calculated from the isotropic chemical shift factors was performed according to Tonelli.⁷ The gauche content varied for the polymers with spacer lengths from 9 to 11 between 22 and 30%. The gauche content could not be calculated from the isotropic chemical shift for poly(1-4) and poly(1-6) because their spacer groups are too short and the chemical shifts are determined mainly by the electronic environment of the neighboring groups. Isotactic poly(1-11) exhibited a moderately higher gauche content in the spacer group than atactic poly(1-11). The atactic polymers showed the well-known odd–even dependence in the transition temperatures and transition enthalpies with significantly lower values in these quantities for poly(1-10) than for either poly(1-9) or poly(1-11) (Table 2). The gauche content in the spacer group of poly(1-10) was also higher than in the spacer groups of poly(1-9) and poly(1-11) (Table 3). The gauche contents found in the spacer groups of the studied polymers are lower than in aliphatic chains attached to stiff macromolecules as side chains,^{8,9} and this indicates a higher degree of conformational order in the flexible spacer. The conformational disorder in the spacer group is also less than in a free polymethylene chain at the corresponding temperature. A simple calculation, based on conformational energies for the gauche and gauche–anti–gauche conformers of 2.1 and 12 kJ/mol with respect to the energy of the trans conformer, shows that the gauche content at 25 °C is close to 36% for a free polymethylene chain. The temperature dependence of the conformational state of the spacer group of poly(1-11) was revealed by the NMR spectra presented in Figure 5. There was an appreciable concentration of gauche conformers in the eleven carbon spacer, as seen from the 32.1 ppm line.

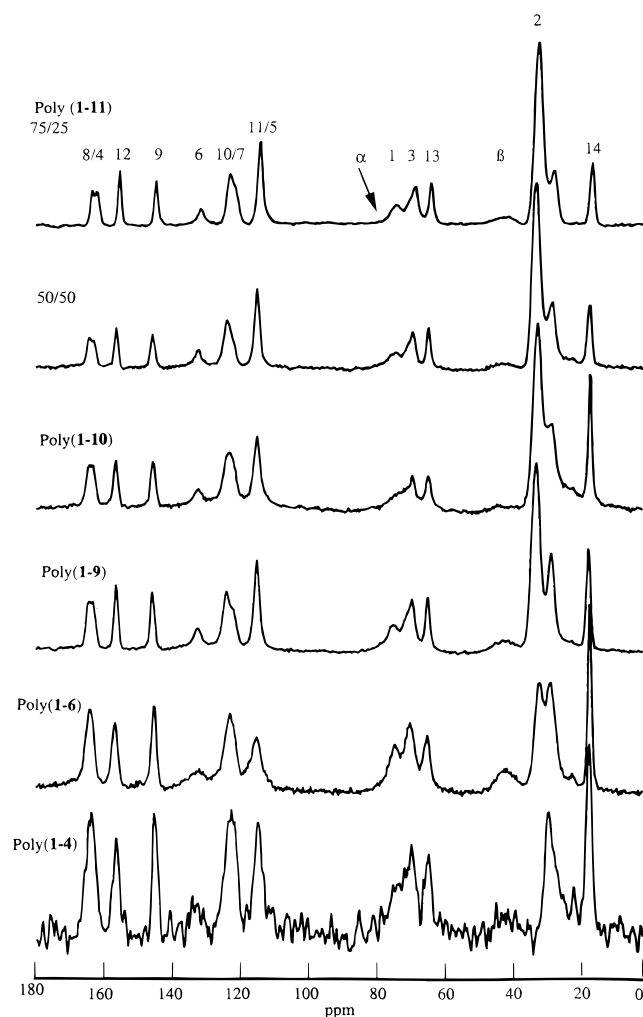


Figure 6. ^{13}C CP MASS TOSS NMR spectra taken at room temperature of poly(1- n) with different spacer lengths (n).

The slight shift of the line by +1.1 ppm in the temperature range from -70°C to $+52^\circ\text{C}$ indicates a moderate change in the gauche content from 20% at -70°C to 30% at $+52^\circ\text{C}$. This change in gauche content is associated with a change in the end-to-end distance of the spacer group of approximately 1 Å. The calculated gauche contents of a free polymethylene chain at these temperatures are 30% (-70°C) and 40% ($+52^\circ\text{C}$).

Figure 6 displays ^{13}C CP MAS TOSS spectra taken at room temperature of the polymers with different tacticities and different spacer lengths. The spectra of the samples with different tacticities were essentially identical (Figure 6). The spectra for polymers with different spacer lengths were mainly influenced so that the isotropic chemical shifts for the aliphatic carbons were changed, presumably due to differences in the electronic environment through the shortening of the spacer.

A selection of isochronal dielectric loss data are presented in Figures 7–9. The studied polymers show a dielectric relaxation behavior conforming to the scheme presented by Gedde et al.¹⁰ a glass–rubber transition (α) and three subglass processes denoted as β (-73°C at 1 Hz), γ (-153°C at 1 Hz), and δ in order of descending temperature. The δ process appeared only as a weak shoulder at -220 to -170°C in the polymers with terminal ethoxy groups at the highest frequencies. The γ process was assigned to local motions within the

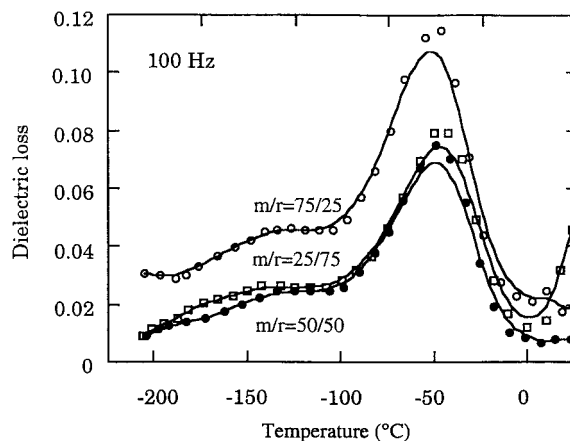


Figure 7. Dielectric loss at 100 Hz as a function of temperature for poly(1-11)s with different tacticities.

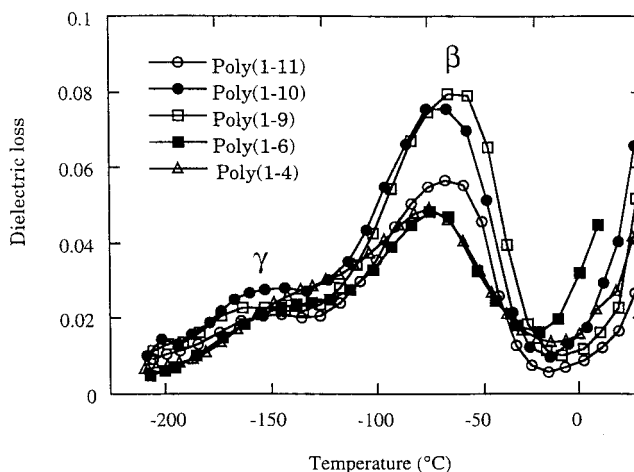


Figure 8. Dielectric loss at 1 Hz for atactic poly(1- n)s with different spacer lengths (n) as a function of temperature:

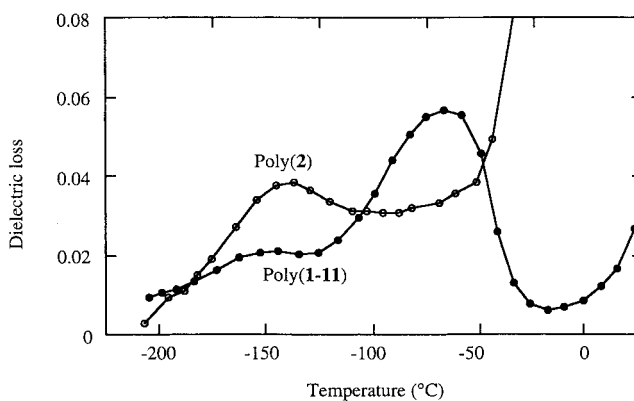


Figure 9. Dielectric loss at 1 Hz as a function of temperature for atactic poly(1-11) and atactic poly(2).

spacer group whereas the β process showed a strong variation in activation energy among the different samples reflecting variations in local order.¹⁰ It was suggested by Gedde et al.¹⁰ that the β process leads to a 180° reorientation of the carboxylic group in the phenyl benzoate moiety accomplished by torsions about the oxygen–carbon atom 4 bond and the oxygen–carbon atom 9 bond (see Figure 1). The two stable conformers (with different orientation of the carboxylic group) have both the carbonyl bond and the inner phenylene in the same plane. The β process involves thus flips of both phenylene rings. It is interesting to compare the flip

Table 4. Activation Energies (ΔE) for Dielectric Relaxation Processes

polymer	$\Delta E(\beta)$ (kJ/mol)	$\Delta E(\gamma)$ (kJ/mol)
poly(1-11), $m/r = 25/75$	106	30
poly(1-11), $m/r = 50/50$	98	31
poly(1-11), $m/r = 75/25$	128	28
poly(1-11D), $m/r = 50/50$	114	30
poly(1-10), $m/r = 50/50$	85	32
poly(1-9), $m/r = 50/50$	84	32
poly(1-6), $m/r = 50/50$	71	42
poly(1-4), $m/r = 50/50$	69	40
poly(2), $m/r = 50/50$		42

dynamics of the inner phenylene group obtained by ^{13}C NMR (0 °C; 60 kHz) and the dielectric β peak. The dielectric data covered only the frequency range 10^{-1} to 10 kHz, but by extrapolation using the Arrhenius equation (validity confirmed in ref 10), it appears that the β peak occurs in the same temperature–frequency range: 0 °C, 50 ± 20 kHz.

Figure 7 and Table 4 show that tacticity played only a minor role in the dielectric relaxation behavior. The peak temperature positions, the activation energies, and the relaxation strengths for both the β and γ processes were essentially the same for the three poly(1-11)s with different tacticities, $m/r = 75/25$, $m/r = 50/50$, and $m/r = 25/75$. The “isotactic” poly(1-11), $m/r = 75/25$, showed an unrealistically high unrelaxed dielectric permittivity and a higher dielectric loss than the other polymers. This is probably an experimental problem associated with the sample cell of this particular sample rather than a problem related to the dielectric properties of the polymer. The polymer with a deuterated backbone (poly(1-11D)) showed the same dielectric relaxation characteristics as the hydrogenated poly(1-11), 0.0607.

The effect of the length of the spacer group on the relaxation behavior is shown in Figure 8. The trend is for the dielectric loss maximum of the β process to pass through a maximum as the spacer length increases. This is probably due to the inability of the mesogen carboxyl group to reorient over the complete three-dimensional space in polymers with short spacer groups. It is further suggested that the reorientation is more complete, i.e., the relaxation strength increases, in polymers with longer spacer groups. There is also a counteracting dilution effect originating from the non-polar spacer group.

Figure 9 shows that the β process does not occur in poly(2), which provides direct evidence for the structural assignment of the β process made earlier.¹⁰ The activation energy of the β process showed a variation between the different samples (Table 4). There is a trend for the activation energy to increase with increasing length of the spacer group. The activation energy of the low-temperature process (γ) was more constant, values between 30 and 40 kJ/mol being obtained. The relaxation strength of the γ process as judged from the size of the dielectric loss peak showed only a moderate variation with spacer length.

Conclusions

Dielectric spectroscopy and solid state ^2H NMR and ^{13}C -MAS NMR spectroscopy of side-chain liquid-crystal-

line poly(vinyl ether)s have provided data on the molecular dynamics. The tacticity has no significant influence on the dynamics at any site in the polymer with a methylene spacer with 11 carbon atoms. ^2H NMR and X-ray diffraction provide evidence for a change in smectic layer thickness, average intermesogenic distance and segmental mobility of the backbone chain accompanying the smectic B–smectic A transition. ^{13}C -MAS NMR data indicated that the gauche content in the spacer group of the polymer with a methylene spacer with 11 carbon atoms was lower than that of a free polymethylene chain at the same temperature and that it increased with increasing temperature. Dielectric spectroscopy confirmed the presence of three subglass processes (β , γ , and δ) obeying the Arrhenius temperature dependence in polymers with phenyl benzoate mesogens. The activation energy (35 ± 5 kJ/mol) of the γ process was insensitive to the morphology, and it is assigned to local motions within the spacer group. The absence of the β process in the polymer with a stilbenzyloxy mesogen suggests that this process is due to reorientation of the carboxylic group in the phenyl benzoate moiety involving flips of the phenylene groups. The frequency of the flip of the inner phenylene unit at 0 °C as obtained by ^{13}C -MAS NMR was almost the same as the frequency of dielectric β loss peak at the same temperature. The relaxation strength associated with the β process passed through a maximum with increasing molar mass the spacer length increases. It is suggested that, in a polymer with a short spacer group, the participating carboxyl group is not able to reorient completely whereas, in polymers with longer spacer groups, reorientation is more complete but the concentration of active mesogens is lower.

Acknowledgment. Financial support from the Axel and Margaret Ax:son Johnson foundation, the Swedish Natural Science Research Council (NFR; K-KU 1910-303), the Polymer Program, Division of Materials Research, National Science Foundation, and the Royal Institute of Technology is gratefully acknowledged. We thank Dr. R. Palmgren, Department of Polymer Technology, KTH, and Dr. C. Möller, Max-Planck-Institut für Polymerforschung, for experimental assistance.

References and Notes

- (1) Spiess, H. W. *Chem. Rev.* **1991**, *91*, 1321.
- (2) Hellermark, C.; Gedde, U. W.; Hult, A. *Polymer* **1996**, *37*, 3191.
- (3) Hellermark, C.; Gedde, U. W.; Hult, A.; Richardson, R. M. *Macromolecules*, submitted for publication.
- (4) Hellermark, C.; Gedde, U. W.; Hult, A. *Polym. Bull.* **1992**, *28*, 267.
- (5) Mopsik, F. I. *Rev. Sci. Instrum.* **1984**, *55*, 79.
- (6) Gray, G. W.; Goodby, J. W. *Smectic liquid crystals- textures and structures* Leonard Hill, London, 1984.
- (7) Tonelli, A. E. *NMR Spectroscopy and Polymer Microstructure*; VCH- Publishers: New York, 1989.
- (8) Clauss, J.; Schmidt-Rohr, K.; Adam, A.; Boeffel, C.; Spiess, H. W. *Macromolecules* **1992**, *25*, 5208.
- (9) Baldwin Frech, C.; Adam, A.; Falk, U.; Boeffel, C.; Spiess, H. W. *New Polym. Mater.* **1990**, *2*, 267.
- (10) Gedde, U. W.; Liu, F.; Hult, A.; Sahlén, F.; Boyd, R. H. *Polymer* **1994**, *35*, 2056.

MA960542U